DECEMBER 02 2003

Characterizing computer cooling fan noise

Lixi Huang

J. Acoust. Soc. Am. 114, 3189–3200 (2003)
https://doi.org/10.1121/1.1624074

Characterizing computer cooling fan noise

Lixi Huang[a)]
Department of Mechanical Engineering, The Hong Kong Polytechnic University, Kowloon, Hong Kong

(Received 23 April 2003; revised 9 August 2003; accepted 4 September 2003)

Computer cooling fan noise is studied theoretically, focusing on the radiation from the interaction between rotor blades and motor struts. The source is decomposed into axial thrust, circumferential drag, and radial force. There is no sound-power coupling among the three components. The index of spatial spinning pressure mode plays the key role in noise radiation. The leading modes are the zeroth, or coincident, mode for thrust and the first mode for the drag and radial force. The effect of source noncompactness is quantified and found to be substantial only for higher-order radiation modes. The sound powers of the leading modes follow a sixth-power law, while the next high-order modes follow an eighth-power law. Quantitative analysis shows that the drag force can be equally noisy as the coincident thrust force. Based on an empirical aerodynamic model of rotor–strut interaction, it is found that the total sound power is more sensitive to the number of struts than rotor blades. Numerical examples are given to demonstrate how the struts can be optimized for typical cooling fan conditions. © *2003 Acoustical Society of America.* [DOI: 10.1121/1.1624074]

PACS numbers: 43.50.Ed, 43.20.Rz, 43.28.Ra [MSH]

Pages: 3189–3200

I. INTRODUCTION

With the increasing maturity of aerodynamic design, acoustic performance is becoming one of the major indices differentiating one manufacturer from another for a broad range of consumer products in which fans are used. The noise radiated by the computer cooling fans is receiving increasing attention as the CPU power increases rapidly and the trend of slim packaging continues. Due to the stringent low budget imposed on cooling fans, technology developed for large fans may not be suitable for computer cooling fans. For example, the technique of active noise control is apparently too costly. A cooling fan is normally manufactured by plastic molding and the tip clearance tolerance in such a small product is usually as large as aircraft engine fans. The much higher clearance-to-fan-radius ratio means a fertile source of noise mechanisms. To the best of the author's knowledge, a comprehensive theoretical study has not been performed for small axial-flow cooling fans.

Research on the general fan aeroacoustics can be said to begin with Gutin's (1936) effort in quantifying the propeller noise caused by the rotation of steady loading, later called Gutin noise. Lighthill's (1952) acoustic analogy provided a formal platform of investigating aerodynamic sound, which was soon extended by Curle (1955) to include the effect of solid boundaries by replacing it with distributed dipoles and monopoles while the explicit effect of acoustic scattering are neglected. It was not until 1969 that Ffowcs Williams and Hawkings (1969) formally extended Lighthill's acoustic analogy by using the generalized functions to account for the effect of solid boundaries in arbitrary motion. The use of the so-called Ffowcs Williams and Hawkings equation became a dominant feature from the late 1970's in the acoustics for rotary machines. Meanwhile, Tyler and Sofrin (1962) revealed the important role played by the numbers of rotor and stator blades, and the phenomenon of modal cutoff consistent with duct acoustics. This analysis represented a major contribution towards turbomachinery acoustics. The link between this cutoff behavior for the ducted fan was related to that of unducted fan by Lowson (1970), whose work also demonstrated that the radiation of mismatched spinning modes cannot be cut off but is rather reduced in acoustic efficiency. Kaji and Okazaki (1970), using the wake models of Kemp and Sears (1953, 1955), modeled the rotor–stator interaction with careful doublet arrays while preserving the blade effects on sound propagation in the duct and imposing Kutta conditions on trailing edges. A comprehensive review was given by Morfey (1973). Meanwhile, Sharland (1964), and Mugridge and Morfey (1972) focused on broadband noise sources for which order of magnitudes estimates were made. In fact, accurate computation of broadband noise is still a challenge, but numerical schemes using elementary experimental data as input can provide useful predictions (Glegg and Jochault, 1998). Longhouse (1976) found that design features good for reducing broadband noise could contradict those for discrete tones. Ffowcs Williams and Hall (1970) showed that trailing edge scattering of turbulent boundary layer flows is a powerful noise source, and the work on this aspect continues today (Howe, 1999) as aerodynamicists are yet to come up with a confident understanding of boundary layer behavior.

In the area of noise abatement for small axial-flow fans, considerable efforts have also been made. A selected few of them are mentioned here. Fitzgerald and Lauchle (1984) demonstrated the effect of a comprehensive range of corrective measures that can be taken to modify a cooling fan design for better acoustic quality. These include the equalization of downstream strut size, the reduction or elimination of the potential flow interaction with nearby objects, use of bellmouth inlet to minimize inlet flow distortions, and the prevention of possible large-scale flow separation on the suc-

a)Electronic mail: mmlhuang@polyu.edu.hk

tion side of blades. Quinlan and Bent (1998) focused on broadband, high-frequency noise generated by the tip leakage flow with extensive acoustic and aerodynamic measurements. Attempts were also made to reduce tonal noise by uneven blades for propellers (Lewy, 1992) and small radial fans (Boltezar *et al.*, 1998). It was concluded that only spectral shifts can be made while the total sound power remains more or less the same. The optimization in terms of stator/vane blade sweep and lean was conducted on advanced ducted propeller (Envia and Nallasamy, 1999) and turbofan engine (Schulten, 1997). The general conclusion is that a stator blade should interact with as many rotor wakes as possible. Similar study has not been found for unducted, small axial-flow fans with few blades. The acoustic feasibility of active noise control for small axial-flow fans was tested using ordinary loudspeakers (Quinlan, 1992) and the fan itself as the secondary source through axial shaking (Lauchle *et al.*, 1997). In both cases a baffle was used, which may have altered the acoustic directivity. The study on propeller noise by Subramanian and Mueller (1995) paid more attention to acoustic directivity. By simulating the acoustic directivity of sound radiated by the fundamental and the first higher-order spinning pressure modes, Gerhold (1997) was able to cancel low-frequency noise of a ducted fan using a ring of orchestrated loudspeakers.

The present study focuses entirely on the tonal noise of isolated computer cooling fans. This represents a first step towards understanding the noise radiation of such cooling fans installed inside a computer chassis. A chassis is a rather confining environment and it would not be surprising that reflection and scattering of sound by confining walls may alter the noise radiation characteristics significantly. However, it might be expected that the chassis environment would not have much scattering job to perform if the sounds radiated by different parts of the fan cancel themselves out in the first place. In other words, efforts in silencing an isolated cooling fan would by no means be wasted. Having said that, the aerodynamic environment inside a computer does present an extra source of noise which is not encountered in free space. For example, the inlet flow is most likely to be nonuniform due to the presence of nearby stationary objects. Apart from the nonuniformity of the potential flow part of the inlet condition, turbulence and deformation of turbulent eddies by a contracting inlet stream tube may also give rise to noise radiation, cf. Trunzo *et al.* (1981) and Majumdar and Peake (1998). Such radiation may contain both broadband (random) and tonal (deterministic) components. For example, the inlet bellmouth of a sample fan shown in Fig. 1(a) has four sharp edges caused by the intersection of the bellmouth and the square outer frame. The inlet flow is expected to have a four-lobe distortion which may or may not contain discrete vortices. The tonal noise induced is expected to be equivalent to the interaction between the rotor blades and a set of four inlet vanes. Most likely, the noise induced by this inlet feature dominates over interaction with other inlet features which are further away from the rotor. The kinematic characteristics of such interaction noise would be similar to that caused by the rotor blades and the downstream struts, the latter being the focus of the present study. In this sense,

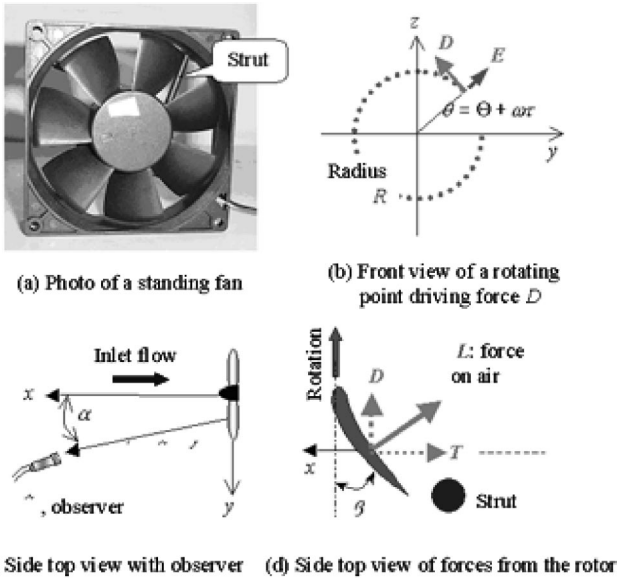

FIG. 1. Sound generated by a rotating force.

the current study deals with the interaction noise inherent in an isolated cooling fan. The interaction is considered to be an unavoidable feature of this category of cooling fans, unlike the freedom Brungart *et al.* (1999) has in their handling of the so-called installation effects for the whole set of vacuum cleaner. In terms of broadband noise, possible sources in the present cooling fan includes the ingestion of inflow turbulence, tip leakage vortex (Fukano *et al.*, 1986), vortex shedding from the rotor blades (Longhouse, 1977), as well as scattering of Tollmien Schlichting waves by the blade trailing edge. The identification and separation of all these possible noise sources are beyond the scope of the current study.

For the typical computer cooling fans, the dominant noise has a typical blade passing frequency (BPF) of 350 Hz for which the fan is physically compact. The effect of blade surface scattering can be ignored and the work of Lowson (1970) is referred to in Sec. II. The dominant noise source is the aerodynamic interaction between the impeller blades and the downstream struts which hold the fan motor. Typical struts are circular or triangular cylinders of small size, and the unsteady forces experienced by the struts are normally much smaller than that on the rotor blades which are, after all, so profiled to generate large lift. Anticipating a possible trend in designing swept and leaned fan, the contribution of the unsteady radial force is, for the first time, included in the formulation. Section III examines the effects of source noncompactness, which is mainly caused by the angular phase distributions instead of physical size. The relative importance of each unsteady force component, thrust, drag, and radial force, is derived analytically for dominant spinning pressure modes. Further progress rests with the spectral knowledge of the rotor–strut interaction force. An empirical model is proposed in Sec. IV with the purpose of investigating the general characteristics of all noise components for various rotor–strut combinations. The current design practices are scrutinized in a quantitative manner with some comparison with experimental results. Numerical examples are then given for a possible optimization of strut design.

II. ELEMENTARY ANALYSIS

Although the details of the point force formulation are available in Lowson (1965, 1970), the noise radiated by the radial component of unsteady force has not been derived. The essential derivation steps are given in this section focusing on the physical interpretation of results and the characterizations appropriate for the computer cooling fan noise. The effect of source noncompactness is investigated in the next section.

A. Point force formulation

As shown in Fig. 1, a typical computer cooling fan consists of a rotor with B blades and S motor struts in its downstream. The struts are typically circular cylinders with a certain leaning angle with respect to the radius to reduce noise, e.g., the fan shown in Fig. 1(a), for which $B=7$, $S=4$.

Using a Cartesian coordinate system (x,y,z) with its origin fixed to the center of a vertically standing fan, the front and side views are shown in the three subfigures of Fig. 1. A cylindrical coordinate system, (x,R,θ), is also introduced and the polar coordinates are shown in Fig. 1(b). For an impeller rotating anticlockwise, the angular coordinate for a point fixed on rotor is given as

$$\theta=\Theta+\omega\tau, \tag{1}$$

where τ is time used for the source, Θ is the initial position of the source point on rotor relative to the stationary reference frame, and ω is the angular speed. No generality is lost if the observer is placed on the horizontal plane, $z=0$, while Θ is allowed to vary. The observer position is denoted by vector $\mathbf{x}=(x_1,x_2,x_3)=(x,y,0)$, and source point by $\mathbf{y}=(y_1,y_2,y_3)$. The distance between them is r and the distance to the origin is defined as r_0. The source is located at $x=x_s$ from the origin and $|x_s|$ is at most comparable to the source radius R. The angular position of the observer, α, is measured from the upstream, as shown in Fig. 1(c). For an observer in the far field, $|x_s|,R\ll r_0$, r can be approximated as

$$r\approx r_0-x_s(x/r_0)-y(R/r_0)\cos\theta. \tag{2}$$

Figure 1(d) shows a blade cross section. The force $\mathbf{F}$ acting on air from a rotating blade is split into three components, thrust force T in the flow direction, drag D in the direction of rotation (the more appropriate term here should be "driving force," but the term "drag" has been used extensively in literature), and radial force E, which can be substantial when the blade leans. The noise radiated by T,D,E is called, respectively, thrust noise, drag noise, and radial noise. The effect of force distribution on the blade surface can be accounted for by the summation of many isolated point forces each with a different initial source position of (x_s,R,Θ) in cylindrical coordinates. For the point force approximation, drag and thrust are related by the pitch angle β

$$T=L\cos\beta,\quad D=L\sin\beta, \tag{3}$$

where L is the airfoil lift. For a fan operating in a condition where the inlet flow is uniform, the unsteady lift on the blade, $L(\tau)$, is mainly produced by the interaction between the moving airfoil and the stationary struts, while the unsteady forces on the struts are produced by a combination of potential and viscous wakes of the rotor. The radial force on a leaning strut can be particularly large. The projection of the total force on the source–receiver direction r is

$$F_r=r^{-1}[-(xT+(ER-x_sT))-yD\sin\theta+Ey\cos\theta], \tag{4}$$
$$\text{(small)}$$

where the contribution from the terms of $(ER-x_sT)$ is small in the far field, $r_0\gg R,|x_s|$, and shall be ignored.

Following Lowson (1965), the sound generated by a rotating point force is

$$p(\mathbf{x},t)=\frac{x_i-y_i}{(1-M_r)c_0r}\frac{\partial}{\partial\tau}\left[\frac{F_i}{4\pi r(1-M_r)}\right], \tag{5}$$

where the right-hand side is evaluated at the radiation time τ, or retarded time, c_0 is the speed of sound, and $M_r=-c_0^{-1}dr/d\tau$ is the Mach number of the source approaching the observer. The Fourier transform of the far-field sound is

$$\begin{aligned}c_n&=\frac{\omega}{\pi}\int_0^{2\pi/\omega}p(\mathbf{x},t)e^{in\omega t}dt\\&=\frac{-\omega}{4\pi^2}\int_0^{2\pi/\omega}\frac{in\omega F_r}{c_0r}e^{in\omega(\tau+r/c_0)}d\tau.\end{aligned} \tag{6}$$

In carrying out the above integration, the leading term of the far-field sound would be retained by substituting r in the denominator by r_0, the same applies to r in F_r given in Eq. (4). But, that in the exponent cannot as it involves the phase angle variation. The phase angle $n\omega r/c_0$ is approximated by

$$\begin{aligned}n\omega r/c_0&\approx nk_0(r_0-x_s\cos\alpha)-nM\sin\alpha\cos\theta,\\M&=\omega R/c_0,\end{aligned}$$

where M is the Mach number of the source rotational speed. Disregarding the mean phase angle corresponding to nk_0r_0, and noting $\omega d\tau=d\theta$, Eq. (6) can be rewritten as

$$\begin{aligned}c_n\approx\frac{-in\omega e^{-ink_0x_s\cos\alpha}}{4\pi^2c_0r_0}\int_\Theta^{2\pi+\Theta}F_r\exp[in(\theta-\Theta\\-M\sin\alpha\cos\theta)]d\theta.\end{aligned} \tag{7}$$

Note that k_0x_s is negligible for small fans, and the term of $e^{-ink_0x_s\cos\alpha}$ is dropped henceforth, although some comments shall be made on this point in the next section. This integration can be evaluated if all force components, denoted as F_j, $j=1,2,3$ for T, D, E, respectively, are Fourier transformed

$$\begin{aligned}F_j&=\sum_{\lambda=-\infty}^{\infty}F_{j\lambda}e^{-i\lambda\omega\tau}\overset{\omega t=\theta-\Theta}{\Rightarrow}\sum_{\lambda=-\infty}^{\infty}e^{i\lambda\Theta}F_{j\lambda}e^{-i\lambda\theta},\\F_{j\lambda}&=\frac{\omega}{2\pi}\int_0^{2\pi/\omega}F_j(\tau)\,e^{i\lambda\omega\tau}d\tau,\end{aligned} \tag{8}$$

in which both positive and negative frequencies are used. The substitution of Eqs. (4) and (8) into Eq. (7) gives

$$c_n \approx \frac{in\omega}{4\pi^2 c_0 r_0} \sum_{\lambda=-\infty}^{\infty} \int_{\Theta}^{2\pi+\Theta} e^{i(\lambda-n)\Theta} \times [T_\lambda \cos\alpha + (D_\lambda \sin\alpha)\sin\theta - (E_\lambda \sin\alpha)\cos\theta] \times \exp[i(n-\lambda)\theta - inM \sin\alpha \cos\theta] d\theta.$$

These integrations lead to the Bessel function of the first kind. Hence

$$c_n \approx \frac{in\omega}{2\pi c_0 r_0} \sum_{\lambda=-\infty}^{\infty} i^{\lambda-n} e^{i(\lambda-n)\Theta} \left[\left(T_\lambda \cos\alpha - \frac{n-\lambda}{nM} D_\lambda \right) \times J_{n-\lambda}(nM\sin\alpha) - (\sin\alpha) i E_\lambda \frac{J_{n-\lambda-1}(nM\sin\alpha) - J_{n-\lambda+1}(nM\sin\alpha)}{2} \right], \tag{9}$$

where the thrust and drag noise terms are identical to those in Lowson (1970). Note that when the rotor does not move, the above formula is no longer valid since the angular position θ used in the expression of F_r in Eq. (4) is no longer related to τ in the time integration of Fourier transform. In other words, one cannot simply substitute $M=0$ into Eq. (9) to find sound generated by stationary struts on which unsteady forces are exerted. Sound generated by one point force on strut can, however, be found through the time-domain formula of Eq. (5), where $M_r=0$ and r is a constant. This procedure is useful when considering sound generated by vortex shedding from struts. When sound is generated by strut experiencing the wake sweeping from the rotor, there is fixed phase relationship among different struts, and the result is similar, though not identical, to Eq. (9) since the source is effectively synchronized with and attached to the rotating blades. The exact formula will be given in the next section.

Since M is very small in computer cooling fans, usually $BM<0.2$, the argument of the Bessel function, $z=nM\sin\alpha$, is very small except for very high frequencies where the source strength has decayed. The following Taylor expansions can be shown to be satisfactory for the range of argument z encountered:

$$J_0(z) \approx 1 - \frac{z^2}{4}, \quad J_\nu(z)|_{|z|\ll|\nu|} \approx \frac{1}{\sqrt{2\pi\nu}} \left(\frac{ze}{2\nu} \right)^\nu. \tag{10}$$

Notice that the second expression works better than the usual approximation of $J_\nu(z) \approx (z/2)^\nu/\Gamma(\nu+1)$ normally adopted for $z\to 0$ for all ν.

It will be shown later that, when the noise made by the interaction between B rotor blades and S struts is taken into account, various acoustic interferences take place. The only possible sound radiated is that given by $n=mB$, $\lambda=kV$, where both m and k are integers. The index of frequency differential, $\nu=n-\lambda$, is the most important parameter controlling how strong a sound component is radiated as it registers mathematically as the order of Bessel functions. As $\nu\to\infty$, the Bessel functions vanish rapidly. This suggests that noise generated by the source component of very different frequencies (Doppler effect) is very low when M is small. For Gutin noise, the source frequency is zero, $\lambda=0$, and the sound-pressure amplitude is $|c_B| \propto J_B(BM) \propto M^B$, which is normally negligible for computer cooling fans. The dominant sound is interaction noise for which ν is small. The following subsection discusses the most typical situations of $|\nu|=0,1,2$ with emphasis on physics related to two factors: one is the change of unsteady force direction as blade rotates; see F_r in Eq. (4), and the other is the change of r during the source motion; see Eq. (2).

B. Modal directivity

The acoustic directivity of the three noise components can be drawn from Eq. (9) by ignoring all constants unrelated to α and by making use of the Bessel function approximations in Eq. (10). The results are shown in Fig. 2 in polar plots of sound intensity with phase angle distribution of sound pressure marked in the lobes, and the simplified expressions given in the vertical labels. Three levels of Bessel function orders are considered, $\nu=n-\lambda=0,1,2$, the results for $\nu=-1,-2$ being similar to $\nu=1,2$. The subfigures in the first row are for thrust noise, the second for the drag noise, and the third for the radial noise. The second row has only two subfigures as the drag noise vanishes for $\nu=0$. First, it is pointed out that thrust noise differs from both drag noise and radial noise. The difference is that the thrust noise has an antiphase relationship when measured in front of and behind the rotational plane, while the drag and radial noises have the in-phase relation across the rotational plane as these two forces lie on the rotational plane. The details of the directivity patterns are analyzed below, while the magnitude of sound power from each noise component is studied in the next section.

For thrust noise, $\nu=0$ can be described as the coincident mode, which means the sound generation at the source frequency itself. The result is a simple dipole in the axial direction, as shown in Fig. 2(a). For $\nu=1$, such as caused by $n=2$, $\lambda=1$, the pattern is shown in Fig. 2(b), similar to that of a lateral quadrupole. This pattern is produced by two factors. One is the dipole nature of the source, which contributes $\cos\alpha$ in the directivity distribution due to the alternating signs of the force projection to the upstream and downstream. The second factor is the motion of the source (Doppler effect). When a force leaves the observer, its effect is equivalent to a decreasing force, and vice versa. The source motion changes r, characterized by $\cos\theta$, and its final effect on sound generation is characterized by $\sin\alpha$. Right on the axis, $\alpha=0,\pi$, r hardly changes when the force circulates, while the change is most dramatic when the observer is on the rotational plane. The combination of $\cos\alpha\sin\alpha$ gives a four-lobe pattern of Fig. 2(b). The second-order radiation ($\nu=2$) is shown in Fig. 2(c) and the pattern can be described as a split dipole.

It can be seen from all subfigures of Fig. 2 that the only possible sound heard on the rotational axis is the coincident thrust noise. The time-domain sound pressure can be found from Eq. (5). In the far field, $r_0 \gg |R|$, F_r does not contain any drag and radial force, and $M_r \approx 0$. The sound becomes

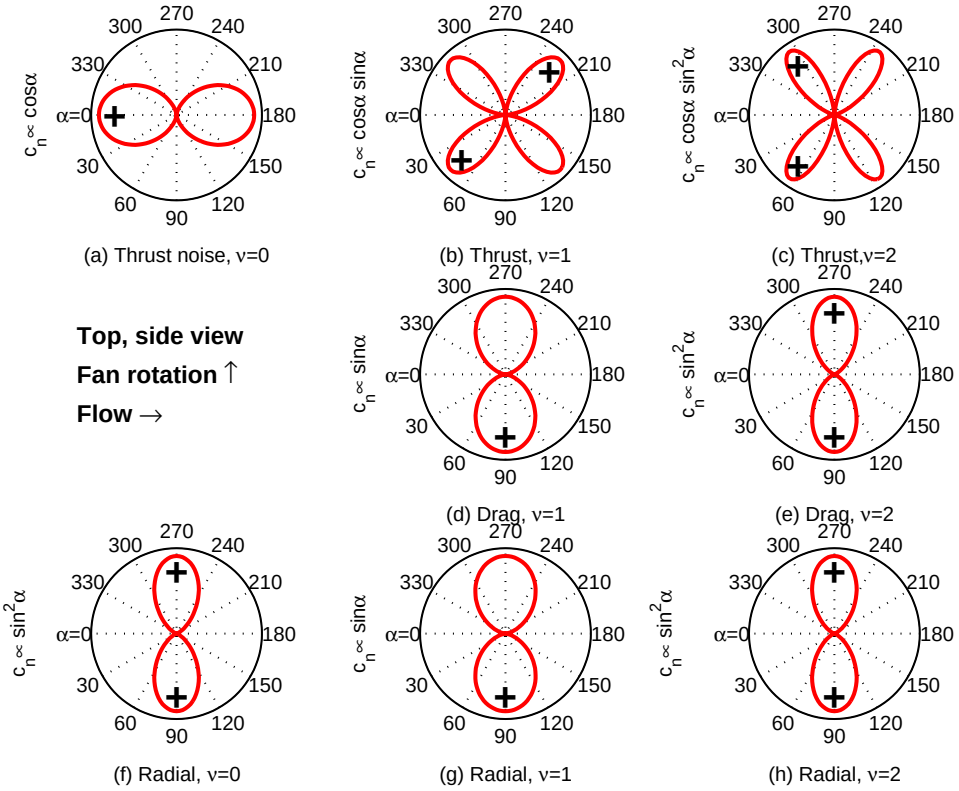

FIG. 2. Acoustic directivity pattern for thrust (top row), drag (middle row), and radial (bottom row) force components. The amplitude is sound intensity, and the symbols of "+" and "−" denote phase angle distribution.

$$p(x,t)\big|_{\alpha=0,\pi} = (\pm 1)\,\frac{\partial T/\partial \tau}{4\pi r_0 c_0}, \tag{11}$$

where the positive sign is for the downstream and negative for the upstream, and thrust T is the total integrated thrust force on all blades at time τ. By measuring the sound on the rotational axis, one can obtain the time-domain characteristics of the lift, $L = T/\cos\beta$, caused by the rotor–strut interaction.

The drag noise is shown in the second row of Fig. 2. The reason why there is no sound at the coincident mode $\nu = 0$ is explained as follows. For source frequency $\lambda = 1$, D changes its sign once between the two halves of a cycle. In other words, D changes direction once when viewed from the rotor. When the blade rotates, the direction of D also changes once relative to the stationary observer. The result is that there is no change of drag force for this particular frequency component; hence, no sound is generated. More explanation is given below when the radial noise is studied. In short, drag noise is generated at all other frequencies due to both force direction change and distance change. The pattern of sound at $\nu = 1$ is given in Fig. 2(d), which is in fact a circulating dipole. The physics is easily appreciated by analyzing what happens for $\lambda = 0$ and $n = 1$. A steady force appears to be an oscillating one when it circulates around. For $\nu = 2$, the pattern shown in Fig. 2(e) differs in phase angle distribution from that of Fig. 2(d). This can be explained easily by looking at $\lambda = 0$, $n = 2$ with the help of Figs. 1(b) and (c). The source trajectory can be divided into two hemispheres, one near the observer and another far from the observer on $z = 0$. When an oscillating D rises from $z < 0$ towards $z = 0$, the force points towards the observer and makes, for instance, a positive sound. The sound made is weak at $\theta = -\pi/2$ due to its distance, but it is also weak at $\theta = 0$ due to the fact that the force is not pointing to the observer despite their proximity. When it moves further up towards $z > 0$, it points away from the observer. The half cycle is converted to one full cycle of sound radiation as $\sin 2\theta$. While D makes positive sound during $\theta = -\pi/2 \rightarrow 0$ to the near-side observer at $y > 0$, it actually makes positive sound to the far-side observer at $y < 0$ as well. This is so because of two factors; one is that drag is pointing away from the far-side observer, hence negative sound, and the other is that it also leaves the observer, hence another negative pressure effect. The combination of the two effects makes a positive pressure oscillation. The result is a pattern shown in Fig. 2(e), which is similar to the far-field directivity of a longitudinal quadrupole.

The sound generated by a moving radial force is similar in pattern as the rotating drag force, as shown in the second and third rows of Fig. 2. However, there are differences in details. The reason why there is radial sound heard at the coincident mode of $\nu = 0$ is explained for the easiest case of $\lambda = n = 1$ and the configuration is shown in Fig. 3. A point source of radial force is circulating with angular position θ. Considering the force signature of $E(\tau) \propto \cos(\theta)$, $\theta = \lambda\omega\tau$, $\lambda = 1$, the force changes direction from outward to inward from $\theta = 0$ to $\theta = \pi$. As a result, the force appears to be in the same direction to a fixed observer when the source is at $\theta = \pi$ as it is at $\theta = 0$. From this perspective, there is little sound generated at the source frequency of $\lambda = 1$. However, due to the difference between the two points to the observer at angular position α, $r_1 < r_2$, there still appears to be pressure variation felt in the far field once per cycle, $n = 1$. The strength is characterized mainly by the Bessel function of

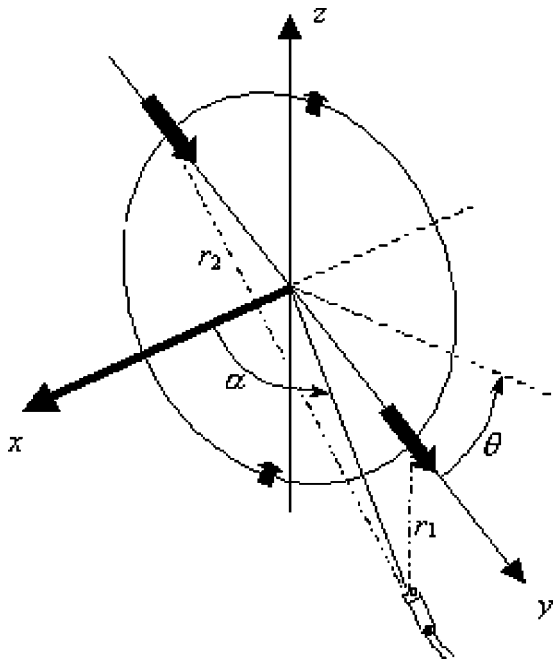

FIG. 3. Sound generation by rotating radial force of the first rotational frequency mode, $\lambda=1$.

$J_{\nu=n-\lambda\pm1}$, which is essentially J_1 when $\nu=0$. This contrasts with the drag noise, which has zero noise generation when $\nu=0$. In the latter case, the highest sound pressure is generated when a drag force passes the point of $\theta=\pi/2$ when D more or less points to the observer located on the plane of $\theta=0$. The sound generated at this point is exactly canceled out by that at $\theta=3\pi/2$ as far as the frequency component $n=\lambda$ is concerned. Of course, there are spectral leaks to other frequencies and the strength of such leak is signified by the Bessel function of order $\nu=n-\lambda$. The difference from the drag noise is that, when $\nu=1$, noise is generated at a magnitude characterized by a Bessel function of zeroth order, for which $J_0(0)=1$. This is explained by using the graph of Fig. 3 and assuming $\lambda=1$, $n=2$. Due to the change of source value once per cycle, i.e., $\lambda=1$, the source force turned inward at $\theta=\pi$, the half cycle of $\theta=0\rightarrow\pi$ actually constitutes one complete cycle of sound radiation. One cycle of drag rotation makes sound at the second harmonic of $n=2$, and the magnitude is characterized by J_0, which implies a high radiation efficiency. In other words, a rotating radial force is actually equivalent to a stationary source of frequency $n=\lambda\pm1$ due to the rotation.

III. ACOUSTIC INTERFERENCE

This section analyzes the total sound power generated by multiple blades and the interaction of sound generated by different force components on blades. Before these are quantified in closed-form formulas using point-force approximation, it is necessary to examine the effect of source noncompactness for different force component and different angular modes.

A. Effect of source noncompactness

The effect of distributed source can be examined by investigating the sum of a series of point forces. The question is how much error is caused by using the instantaneous average of the force components, $F_j(\tau)$, in computing the Fourier transform of Eq. (8), instead of summing the acoustic contribution from each point force given in Eq. (9). A proper integration over the distributed source involves putting right two factors. One is the source position, and the other is the phase angle relationship. The effect of the axial source position x_s is clearly seen in the term of $\exp(-ink_0x_s\cos\alpha)$ in Eq. (7). The error involved in approximating $x_s=0$ for all source points is proportional to nk_0x_s, which is essentially the ratio of the axial extent of the source to the wavelength of frequency $n\omega$. For compact cooling fans, this can be ignored.

The effect of varying the angular position of the source, Θ, manifests itself as $e^{i(\lambda-n)\Theta}$ in Eq. (9) for all three force components in cylindrical coordinates, denoted as $F_j(\tau), j=1,2,3$ for $T(\tau),D(\tau),E(\tau)$, respectively. In time domain, this means that the distributed surface pressure, $p(\Theta,\tau)$, should be integrated over the blade surface S as a lumped component force, denoted as $\tilde{F}_j(\tau)$, with a time delay of $\Theta(\lambda-n)/(\lambda\omega)$. The pair of time-delayed integration and its Fourier transform, denoted as $\hat{F}_{j\lambda}$, are given below

$$\tilde{F}_j(\tau)=\int_S p\left(\Theta,\tau-\frac{\Theta(\lambda-n)}{\omega\lambda}\right)n_j\,ds,$$

$$\hat{F}_{j\lambda}=\frac{\omega}{2\pi}\int_0^{2\pi/\omega}\tilde{F}(\tau)e^{i\lambda\omega\tau}d\tau=\int_S e^{i(\lambda-n)\Theta}\hat{p}_\lambda n_j\,ds, \quad (12)$$

$$\hat{p}_\lambda=\frac{\omega}{2\pi}\int_0^{2\pi/\omega}p(\Theta,\tau)e^{i\lambda\omega\tau}d\tau,$$

where n_j is the component of unit normal vector in the cylindrical coordinate system.

When $n=0$, the time delay is exactly what is required to rewind the source back to $\Theta=0$. In other words, $\tilde{F}_j$ is simply the sum of forces at the different times when they pass through a fixed point in space. For coincident noise, $n=\lambda$, no time delay is needed and the instantaneous force integration gives the correct prediction. For other n, the amount of time delay varies. For $n>\lambda$, time advance occurs. There is no universal time-delay-integration scheme that can capture all frequencies correctly using a lumped source in the circumferential direction.

However, it is normally sufficient to focus on one dominant noise source index for which $|n-\lambda|=0,1,2$. For the example of $B=7$, $S=4$, it can be shown that $\lambda=2S=8$ is the dominant source frequency index, so that a time delay of $\Theta/8\omega$ is suitable for the BPF noise. In this case, the effect of approximating $\tilde{F}_j(\tau)$ by an instantaneous spatial integration is expected to lead to some errors. Two typical cases are considered for error analysis with reference to the blade diagram shown in Fig. 1. In the first case, unsteady flow pressure p on the rotor blade is assumed to have the same phase angle but with a linearly decaying magnitude with respect to

the chordwise coordinate of $\xi \in [0,C]$, where $\xi=0$ means the trailing edge. Denoting the instantaneous integration of force F_j by G_j, one has

$$p(\xi,\tau)n_j = 2A_\lambda e^{-i\lambda\omega\tau}(1-\xi/C),$$

$$G_j(\tau) = \int_0^C p(\xi,\tau)\, n_j\, d\xi = A_\lambda C e^{-i\lambda\omega\tau},$$

$$\hat{G}_{j\lambda} = \frac{\omega}{2\pi}\int_0^{2\pi/\omega} G_j(\tau) e^{i\lambda\omega\tau} d\tau = A_\lambda C.$$

The approximate complex sound amplitude is then $c_n' \propto A_\lambda C$, while the accurate sound is found by integrating $e^{i(\lambda-n)\Theta}\hat{F}_\lambda$ in Eq. (9) over the chord where Θ varies from 0 to ϕ

$$\hat{F}_\lambda(\xi) = 2A_\lambda(1-\xi/C),$$

$$c_n \propto \int_0^C \hat{F}_\lambda(\xi) e^{i(\lambda-n)\Theta}\, d\xi = A_\lambda C\left[\frac{1+i(\lambda-n)\phi - e^{i(\lambda-n)\phi}}{[(\lambda-n)\phi]^2/2}\right].$$

The square bracket represents the deviation of the true amplitude c_n from the approximate one, c_n'. Taking the following parameters as an example, $\lambda=8$, $\phi=2\pi/10$, the ratio of the two amplitudes is 0.99, which is very satisfactory.

In the second case, the unsteady forces on the rotor are still assumed to decay linearly from the trailing edge where interaction takes place, but the pressures are related by time delays according to the rotation

$$p(\xi,\tau)n_j = 2A_\lambda(1-\xi/C)e^{-i\lambda(\omega\tau+\Theta)},$$

$$G_j(\tau) = \int_0^C p(\xi,\tau)n_j\, d\xi = A_\lambda C\,\frac{1-i\lambda\phi-e^{-i\lambda\phi}}{(\lambda\phi)^2/2} e^{-i\lambda\omega\tau},$$

$$G_{j\lambda} = A_\lambda C\,\frac{1-i\lambda\phi-e^{-i\lambda\phi}}{(\lambda\phi)^2/2},$$

$$c_n' \propto A_\lambda C\,\frac{1-i\lambda\phi-e^{-i\lambda\phi}}{(\lambda\phi)^2/2}.$$

The accurate sound is

$$\hat{F}_\lambda(\xi) = 2A_\lambda(1-\xi/C)e^{-i\lambda\Theta},$$

$$c_n \propto \int_0^C \hat{F}_\lambda(\xi)\, e^{i(\lambda-n)\Theta} d\xi = A_\lambda C\left[\frac{1-in\phi-e^{-in\phi}}{(n\phi)^2/2}\right].$$

The ratio of approximate to accurate sound for the example is

$$\frac{c_n'}{c_n} = \left[\frac{1-i\lambda\phi-e^{-i\lambda\phi}}{1-in\phi-e^{-in\phi}} \times \frac{n^2}{\lambda^2}\right],$$

which is 0.8366 or 1.55-dB error. The error grows fast for higher order modes, e.g., $|\nu|=2$.

The radial noncompactness manifests itself through the rotational Mach number, $M=\omega R/c_0$. For the thrust noise, the effect depends on the order $\nu=n-\lambda$. For the coincident mode, there is essentially little influence since $J_0(z)\approx 1-z^2/4\to 1$ for small $z=nM\sin\alpha$. For other modes, $J_\nu(z)\propto z^\nu$. The error caused by placing the lumped source at a radius where the load peaks is easily estimated. The drag noise has different characteristics. The dominant noise comes from when $\nu=\pm 1$ when the Mach number actually does not matter as $J_1(nM\sin\alpha)/M$ is almost constant when M is small. The second-order drag noise features $D_\lambda J_2(nM\sin\alpha)/M \propto DR$, so that the noise radiated is proportional to the integrated torque. The dominant radial noise also comes from $\nu=1$ and the Bessel function involved is $J_0(nM\sin\alpha)$ which is also immune from the variations of the Mach number. In summary, the error caused by lumping forces at an inappropriate radius depends on the dominant noise-making mode. The error will be negligible for all the leading radiation modes.

The summation of sound made by multiple blades is done by assuming that pressure fluctuation caused by the rotor–strut interaction occurs when a blade passes through an arbitrary fixed strut position; hence, the fixed phase angle distribution among all forces on all blades. As was shown by Lowson (1970), the summation of sound from B evenly spaced blades interacting with S evenly spaced struts is

$$c_{n=mB}^{(\text{rotor})} = \frac{imB^2S}{2\pi c_0 r_0}\sum_{k=-\infty}^{\infty} i^{-\nu}\left\{\left(T_{kS}\cos\alpha - \frac{\nu}{nM}D_{kS}\right)\times J_\nu(nM\sin\alpha) - \frac{i}{2}(\sin\alpha)\times E_{kS}[J_{\nu-1}(nM\sin\alpha) - J_{\nu+1}(nM\sin\alpha)]\right\}, \quad \nu = mB-kS, \tag{13}$$

where T_{kS}, D_{kS}, E_{kS} are derived from the encounter of a single blade with a single strut. Similarly, the sound from struts is found to be of the same form as Eq. (13) except that the subscripts of kS in the forces are changed to mB as there is no Doppler effect from stationary sources, although a pattern of acoustic interference exists

$$c_{n=mB}^{(\text{strut})} = \frac{imB^2S}{2\pi c_0 r_0}\sum_{k=-\infty}^{\infty} i^{-\nu}\left\{\left(T_n\cos\alpha - \frac{\nu}{nM}D_n\right)\times J_\nu(nM\sin\alpha) - \frac{i}{2}(\sin\alpha)\times E_n[J_{\nu-1}(nM\sin\alpha) - J_{\nu+1}(nM\sin\alpha)]\right\}, \quad \nu = mB-kS. \tag{14}$$

B. Sound-power integrations

The sound-power integration for each frequency index $n=mB$ is

$$W_n = \int_0^\pi \frac{|c_n|^2}{2\rho_0 c_0} 2\pi r_0^2 \sin\alpha d\alpha, \tag{15}$$

where complex $c_{n=mB}$ is given in Eqs. (13) and (14). For the same sound frequency of index $n=mB$, there are acoustic interferences among sounds generated from different source frequencies (due to the Doppler effect) and among sounds

from different force components at the same frequency. Analytical progress is only possible by considering the dominant order of $\nu = n - \lambda$ for each force component, and by assuming that the three force components of the same frequency share the same phase angle as they are all related to the same unsteady pressure normal to the local blade surface.

As shown in Eq. (10), the Bessel functions decrease rapidly with the order ν, $J_\nu(z) \propto z^\nu$, the order with lowest $|\nu|$ is dominant, and only the dominant order is necessary as the typical value of argument $z = nM \sin\alpha$ is much less than unity for typical cooling fans. For a moderately high value of $z = 0.5$, the ratio of $J_{\nu+1}(z)/J_\nu(z)$ is 0.2582,0.1263, 0.0838,0.0627 for $\nu = 0,1,2,3$, respectively. The highest ratio of 0.2582 means a 11.8-dB difference, which is considered to be large enough. When considering the drag noise, however, the acoustic amplitude is proportional to $\nu J_\nu(z)$ and the ratio $(\nu+1)J_{\nu+1}(z)/[\nu J_\nu(z)]$ is 0.2526,0.1257,0.0836 for $\nu = 1,2,3$, respectively. Having said that, the error caused by neglecting the acoustic interference between a sound of amplitude 1 and another of amplitude 0.25 can be as big as $20\log_{10} 1/0.75 = 2.5$ dB. The maximum possible error will be reduced to about 1.1 dB for a smaller value of $z = 0.25$.

The presence of i in the radial noise term iE_{mB} in Eqs. (13) and (14) means that the radial noise is 90 deg out of phase with the thrust and drag noise in time domain, hence no interference. The interference between the thrust and drag noise for the dominant order ν is illustrated as

$$c_n = (aT_\lambda \cos\alpha + bD_\lambda)\sin^\nu \alpha,$$

where a and b are both real quantities, and the asymptotic formula of Eq. (10) has been employed. The sound power integration, Eq. (15), gives zero coupling between $T_\lambda D_\lambda$

$$W_n \propto \int_0^\pi (aT_\lambda \cos\alpha + bD_\lambda)^2 \sin^{2\nu+1}\alpha d\alpha$$

$$= C_T(\nu)a^2T_\lambda^2 + C_D(\nu)b^2D_\lambda^2,$$

$$C_T(\nu) = 2\int_0^1 x^2(1-x^2)^\nu dx,$$

$$C_D(\nu) = 2\int_0^1 (1-x^2)^\nu dx.$$

To conclude, the sound power contributed by $T_\lambda, D_\lambda, E_\lambda$ can be calculated individually and simply added up, the results being

$$W_n = \frac{(nBS\omega)^2}{4\pi\rho_0 c_0^3}[T_\lambda^2 W_{n\lambda}^{(T)} + D_\lambda^2 W_{n\lambda}^{(D)} + E_\lambda^2 W_{n\lambda}^{(E)}], \quad \nu = n - \lambda,$$

$$\mu = \frac{nM}{4},$$

Mode\Power	$W_{n\lambda}^{(T)}$	$W_{n\lambda}^{(D)}$	$W_{n\lambda}^{(E)}$
$\nu = 0$:	2/3	0	$5.02\mu^2$
$\nu = \pm 1$:	$1.25\mu^2$	0.392	1/3
$\nu = \pm 2$:	$0.667\mu^4$	$1.16\mu^2$	$1.25\mu^2$

(16)

where the new parameter $\mu = nM/4$ is introduced purely for the convenience of comparative study as most coefficients are then close to unity. Several observations are made.

(i) For coincident condition of $\nu = mB - kS = 0$, noise is mainly made by the unsteady thrust.

(ii) For the first rotational mode of $\nu = \pm 1$, the drag noise dominates over thrust noise in terms of noise-making ability. If one assumes a pitch angle of $\beta = 30°$, as shown in Fig. 1, and $nM = 0.5$, $T_\lambda = \sqrt{3}D_\lambda$, but still the drag noise is 14.3 and 8.3 dB higher than the thrust noise for $nM = 0.25,0.5$, respectively.

(iii) For the higher order $\nu = \pm 2$, the noise-making ability of all force components is reduced. The dominance of drag noise over thrust noise is even more pronounced. The physics of such dominance originates from the fact that rotating drag radiates noise by its rapid change of direction, while rotating thrust through its changing distance to the observer.

(iv) The radial noise is about the same as the drag noise for $\nu = \pm 1$ if $E_\lambda = O(D_\lambda)$, and its radiation ability at $\nu = 0$ is exactly 4 times higher than that at $\nu = 2$.

(v) Source radius R enters the expression through the rotation Mach number M. When the sound-power dependency does not contain M, the location of the source does not matter and the acoustic radiation is considered to be of the leading mode. This occurs for $\nu = 0$ in the thrust noise, $|\nu| = 1$ for the torque and radial noise, and the term ''leading'' is meant to differentiate from the ''coincident'' condition of $\nu = 0$. In these cases, the radial location of the source does not matter as far as the distributed forces are lumped properly in time domain if it occupies a significant portion of the circumference.

(vi) When the power dependency contains $(nM)^2$, the radius of the source point is coupled with the fluctuating forces. For drag D at $|\nu| = 2$, this makes a perfect expression for torque. For thrust noise at $|\nu| = 1$, it constitutes a bending moment, while that for the radial force does not have an obvious physical attribute. The drag noise should be renamed torque noise, but it is of secondary importance in terms of sound power. These modes are collectively called secondary modes, or simply higher-order modes.

(vii) If the modal coefficients of the unsteady forces, $T_\lambda, D_\lambda, E_\lambda$ are assumed to be proportional to the mean flow speed, the power dependency for a given geometrical shape can be expressed as $W \propto M^6R^2W_{n\lambda}^{(T,D,E)}$, where $W_{n\lambda}^{(T,D,E)}$ represents the dimensionless power from the three force components. For the leading mode radiation, $W_{n\lambda}^{(T,D,E)}$ is constant, so that the power exponent is 6. For secondary mode radiation, it becomes at least 8, depending on the exact circumferential order ν and force component concerned. In reality, the tonal sound is often superimposed on a broadband noise which could originate from the trailing edge scattering, which was shown by Ffowcs Williams and Hall (1970) to have a power dependency exponent of 5. The exponent for the total sound power is often between 5 and 6, which is well known empirically.

(viii) The exact parametric relationship for each component noise cannot be made explicit until theoretical models

are established to relate these force components with design parameters of B,S,ω,R as well as other features of the fan assembly. Mechanisms of lift fluctuation is better understood than those for fluctuating radial forces. However, it may be speculated that significant fluctuations of radial forces could arise from the blade tip and casing due to the motion of tip vortices. Another possible significant source is the leaning design of stator/struts for the purpose of causing destructive acoustic interference of thrust and drag noise.

IV. AERODYNAMIC INTERACTION MODEL

If the lift experienced by a rotor blade passing over S struts is S triangular pulses of height C_L, including rising and falling legs of equal time duration, and each occupies an angular width of $2\pi/S_L$, $S_L>S$, the Fourier component of the lift, L_λ, is found as follows:

$$L_{\lambda=kS}=\frac{S_L C_L}{S\pi^2 k^2}\left(1-\cos\frac{k\pi S}{S_L}\right),$$

where high S_L means short pulses typical of radial struts aligned with the trailing edges of the rotor blades. Although $S_L>S$ would normally be the case, S_L should be independent of S as the former describes the interaction between one rotor blade and one stator blade. Note that the oscillation term of $1-\cos(k\pi S/S_L)$ is associated with the precise pulse shape of rising and falling edges and their slopes, and the term disappears when the pulse has a parabolic shape. In general, it is difficult to determine the precise pulse shape; it would therefore be of more general value if the following relationship is assumed:

$$L_{\lambda=kS}=C_L/(Sk^2). \tag{17}$$

Here, C_L depends purely on the kinematics of how a strut interacts with blade rows, and it has also contained the effect of the pulse duration S_L. It is anticipated that a strut with considerable lean would have lower C_L in general, but surely C_L is not related to B or S. It is also noted that the model is only of limited value when it comes to the comparison of sounds generated at different BPFs since the potentially important oscillation term has been ignored. Note also that, when the individual rotor blade and strut encounter produces a very sharp pulse, the spectrum of unsteady lift approaches that of white noise, and the factor of k^{-2} in Eq. (17) would approach a constant, k^0.

Theoretically, the exact lift waveform can be measured by listening to the sound on the rotational axis, according to Eq. (11). A special configuration has to be made so that the rotor–strut interaction occurs simultaneously for all blades as $T(\tau)$ is the summation of thrust on all blades. Whether the result for such a special configuration can be applied to different combinations of B and S is uncertain.

In most cases, estimates of the unsteady radial forces are not available, radial noise is temporarily set aside. This leaves the thrust and drag noise. The thrust and drag forces are related to the lift by the pitch angle β. When k is replaced by $k=(n-\nu)/S$, and Eq. (17) is substituted into Eq. (16) for thrust and drag noise, the sound power of the mth BPF harmonic is rewritten as

$$W_m^{(TD)}=\frac{W_{n=mB}}{C_l}=\left(\frac{S}{1-\nu/n}\right)^4\left[\frac{W_{n\lambda}^{(D)}+W_{n\lambda}^{(T)}\tan^{-2}\beta}{m^2}\right],$$

$$C_l=\frac{(\omega C_L\sin\beta)^2}{4\pi\rho_0 c_0^3}, \tag{18}$$

where C_l is related to the unsteady lift coefficient and can be treated as a constant in the following discussions.

For the leading noise radiating modes, $\nu=0$ for thrust and $|\nu|=1$ for radial and drag noise, $W_{n\lambda}^{(T)}$ and $W_{n\lambda}^{(D)}$ are constants. This means that the strut number S plays a dominant role as $W_n\propto S^4$, while the rotor blade number does not feature in the power expression at all. For secondary modes, the power coefficients, $W_{n\lambda}^{(T,D)}$, contain μ^2, where $\mu=mBM$, so that B enters the sound-power expression as B^2, which is still less important than S^4. Note that B^2 would also appear in the noise power expression for the leading noise radiation modes if k^{-2} in the scaling law of Eq. (17) is replaced by k^{-1}.

The number of struts is determined partly by structural considerations. Given the power dependence of S^4, focus is therefore put on designs with small S. $S=2,3,4,5$ are all possible designs.

A. Analysis of typical cooling fan

The most typical design shown in Fig. 1(a) has $B=7$ rotor blades and $S=4$ struts behind the impeller. The particular fan in the photo has a hub and tip diameters of 37 and 86 mm, respectively. When it is operated at 3000 rpm in the free-delivery condition, the volume flow rate is around 0.03 m^3/s, while the maximum total pressure rise is about 50 Pa when it is fully blocked. The fan itself has one strut larger than the other three for carrying electric wiring. When this extra size is trimmed, the sound power is found to be 45 dB re: 10^{-12} W. The first 3 BPFs have a sound-power distribution of 44.8, 23.8, 31.0 dB. Details of the experimental setup are described in Wong and Huang (2003).

For this combination of B and S, $\nu=B-2S=-1$ is the dominating mode for the fundamental BPF. For the purpose of analysis, point force is assigned to be where the maximum steady flow loading normally occurs, such as 80% of the tip radius, $R=3.4$ cm, for which $BM\approx0.22$, $\mu=nBM/4=0.055,0.11,0.16$ for $m=1,2,3$, respectively. The pitch angle is assumed to be $\beta=30°$, $\tan^{-2}\beta=3$. Using Eq. (18), the comparison of sound radiating ability of drag and thrust noise is found as follows:

$$W_{n\lambda}^{(T)}=1.25\mu^2=0.0038,\quad W_{n\lambda}^{(D)}=0.392,$$

$$\frac{W_{n\lambda}^{(D)}}{W_{n\lambda}^{(T)}\tan^{-2}\beta}=34.4,$$

which means a difference of 15.4 dB. Despite the fact that thrust force component is 1.73 times larger than the drag force, the dominant noise source is still the drag noise as this is the leading radiation mode. Most radial noise would be

radiated from the strut and it is simply assumed here that it is also much less than the drag noise.

Despite the uncertainties associated with the Fourier transform of the rotor–strut interaction force in Eq. (17), the second and third harmonics are still estimated as follows for reference. The leading modes are $\nu = mB - kS = -1$ for the first BPF as $k=2$. For the second BPF, both $k=3$ gives $\nu = 2$ and $k=4$ gives $\nu = -2$. Both are secondary radiating modes, and their coupling effect cannot be determined unless the interaction force is measured. If their amplitudes are similar and they interfere constructively, the outcome could be a sound power 4 times higher than the estimate based on one of them. Bearing this uncertainty in mind, the estimate now proceeds for $k=3$ as it is likely to have a higher amplitude according to Eq. (17). For the third BPF, $\nu = 3B - 5S = 1$ is the only contributing mode. For all three frequencies, drag noise dominates. By inserting the various values of ν and ignoring the term $W_{n\lambda}^{(T)}$ in Eq. (18), one has

$$W_{m=1}^{(TD)} = 58.8, \quad W_{m=2}^{(TD)} = 1.7, \quad W_{m=3}^{(TD)} = 13.6,$$

$$\Sigma_{m=1}^{3} W_m^{(TD)} = 74.0;$$

$$\frac{W_{m=1}^{(TD)}}{W_{m=2}^{(TD)}} = 35.3, \quad (15.4 \text{ dB}); \quad \frac{W_{m=1}^{(TD)}}{W_{m=3}^{(TD)}} = 4.3, \quad (6.4 \text{ dB}).$$

Compared with experimental results, both the second and the third BPF are overpredicted, but the prediction that the third BPF is higher than the second agrees with the prediction. The numerical discrepancy can arise from many factors assumed in the interaction model of Eq. (17), which is only expected to give a general trend of force spectrum.

B. Effect of reduced number of struts

Using the above result as the reference case, it would be interesting to see how such sound power compares with the coincident thrust noise for $B=6$, $S=2$. In this case, $\nu = B - 3S = 0$, and $W_{n\lambda}^{(T)} = 2/3$. It is found that $W_{m=1}^{(TD)}|_{B=6,S=2} = 32.0$, which is still lower than the drag noise of the reference case. This example serves to highlight the equal importance of the leading drag noise and thrust noise at the coincident mode of $\nu = 0$. Having said that, the problem with the design of $B=6$, $S=2$ is that there is coincidence thrust noise at all higher harmonics.

The second case to be considered is $B=7$, $S=2$. Since coincidence occurs at the second harmonic, another case $B=7$, $S=3$ is also considered, which brings a third harmonic coincidence. As comparison varies from one harmonic to another, the first three harmonics are considered together for the total sound power

	$m=1$	2	3	$\Sigma_{m=1}^{3}$
$W_m^{(TD)}\|_{B=7,S=2}$	11.6	8.0	0.8	20.5
$W_m^{(TD)}\|_{B=7,S=3}$	58.8	0.2	18.0	77.0.

The better design seems to be $B=7$, $S=2$, which is predicted to radiate $10\log_{10}(74.0/20.5) = 5.6$ dB less noise than the reference case. However, there is a likelihood that structural weakness may require a large strut, and the predicted noise-power reduction may not be fully realized. It must be emphasized that, with such few struts, most harmonics are radiated by the leading modes of $\nu = 0, \pm 1$.

All the cases considered so far have a BPF noise radiated by the leading mode. The last case to be considered is $B=7$, $S=5$, for which the BPF noise is given by $\nu = 2$. The dominating modes are considered for six harmonics as follows:

$$\nu_{m=1} = B - S = 2, \quad \nu_{m=2} = 2B - 3S = -1,$$

$$\nu_{m=3} = 3B - 4S = 1,$$

$$\nu_{m=4} = 4B - 6S = -2, \quad \nu_{m=5} = 5B - 7S = 0,$$

$$\nu_{m=6} = 6B - 8S = 2,$$

$$W_{m=1\to 6}^{(TD)} = 8.4, \quad 46.5, \quad 33.1, \quad 1.7, \quad 50.0, \quad 2.7;$$

$$\Sigma_{m=1}^{3}: 88.0; \quad \Sigma_{m=1}^{6}: 142.3.$$

Here, the fifth harmonic dominates despite the natural decay with m. This prediction may not materialize in practice as the phase angle of forces may not be so well synchronized on all blades at very high harmonics due to uncertain aerodynamics of vortex shedding, etc. From the point of view of prediction, the sum of the first three harmonics amounts to the similar level of power as the reference design, which represents a trade-off between the increased S and increased ν for the fundamental BPF. As a summary, the optimal design for $B=7$ seems to be $S=2$ according to the interaction model of Eq. (17).

V. CONCLUSIONS

(1) Unsteady forces can be conveniently separated into axial thrust, circumferential drag, and radial force. Thrust noise radiates efficiently when the number of rotor blade coincides with the struts as $\nu = mB - kS = 0$, but the drag noise and radial noise peaks at the first mode of $\nu = \pm 1$ with very similar radiation efficiency. The traditional design of $\nu = \pm 1$ is thus questionable. The leading radiation mode of drag/radial forces changes from $\nu = 0$ to $\nu = \pm 1$ due to the constant change of force direction. The modes of $|\nu| = 1$ for thrust and $|\nu| = 2$ for drag/radial forces are regarded as secondary as they radiate much less noise. In terms of noise-power law with regard to the fan rotational speed, the leading modes have a sixth-power law, while the secondary modes have an eigth-power law.

(2) Radial noise is formulated for the first time, and is shown to be 90° out of phase with the thrust and drag noise if the force derived from one physical source. The natural radiation mode is also $\nu = \pm 1$. Unlike drag noise, it also radiates at $\nu = 0$. Little has been done or known about this noise component. It is speculated that significant radial noise can be present where tip vortices are strong and structural irregularities exist near the tip regions of the struts and rotor blades.

(3) It is shown analytically that there is no sound radiation power coupling among the three force components as they are orthogonal to each other. Thrust noise and drag noise are separated by directivity differences, while ra-

dial noise and thrust/drag noise can be separated by phase differences. The total sound power at the same frequency is the sum of three component sounds.

(4) The effects of source noncompactness have been quantified. The axial noncompactness is normally negligible for cooling fans operating at low tip speed. In the radial direction, it is also possible to lump the forces at one radius without losing any accuracy. For the leading mode of $\nu=0$ for thrust and $\nu=\pm 1$ for drag/radial noise, the radial position of the forces does not matter. For the secondary modes of $|\nu|=1$ for thrust and $|\nu|=2$ for drag/radial forces, the first-order moment of these forces should be found. For the drag force, the moment is exactly torque. For the thrust force, it becomes the bending moment. An effective mean radius can thus be defined.

(5) In the circumferential direction, no fan is too small to be noncompact. The noncompactness should be overcome by lumping distributed force with a time-delayed integration of distributed force on the circumference, and the time delay required takes the form of $p(\Theta,\tau-\Theta(\lambda-n)/(\lambda\omega))$, where Θ is the angular coordinate of the distributed force. For $\nu=n-\lambda=0$, no time delay is needed. For $n=0$, the time delay means rewinding the blade back to a fixed point in space. For intermediate modes of $\nu=-1,-2,\ldots$, a small amount of backwinding is required, while for $\nu>0$, time advance occurs. As different time delay is required, no universal spatial-averaging scheme can be devised for point-force representation. However, it is generally sufficient to tackle the leading radiation modes, for which the required time delay is small and the simultaneous force integration suffices.

(6) Acoustic directivity patterns are identified for thrust, drag, and radial noise. Thrust noise has the distinct four-lobe pattern when radiating at the noncoincident mode, while a unique axial two-lobe pattern is formed when it operates at the coincident mode. This noise component can be easily separated from the rest by taking the upstream–downstream differential measurement. Drag noise and radial noise cannot be distinguished from the directivity pattern, but their separation could be devised in time-domain operations provided that the radial force and circumferential force originate from the same surface pressure fluctuation on blade surfaces. The interaction of thrust noise with drag/radial noise would create a variety of acoustic directivity.

(7) Acoustic optimization has to rely on detailed knowledge of the fluctuation pressure signature caused by the encounter between one rotor blade and one strut. When the encounter produces a sharp pulse, the radiated noise is expected to be rich in higher harmonics, and the number of rotor blades is expected to be important for the total sound power. If, however, the encounter produces a broader waveform signature with rapid spectral roll-off, the number of struts is expected to be the dominant factor. For the particular example of seven-blade rotor, a design of two strut is predicted to radiate much less noise than a four-strut design.

ACKNOWLEDGMENT

The project is funded by a Competitive Earmarked Research Grant from the Hong Kong SAR Government (PolyU 5162/01E).

Boltezar, M., Mesaric, M., and Kuhelj, A. (**1998**). ''The influence of uneven blade spacing on the SPL and noise spectra radiated from radial fans,'' J. Sound Vib. **216**, 697–711.

Brungart, T. A., Lauchle, G. C., and Ramanujam, R. K. (**1999**). ''Installation effects on fan acoustic and aerodynamic performance,'' Noise Control Eng. J. **47**, 3–7.

Curle, N. (**1955**). ''The influences of solid boundaries upon aerodynamic sound,'' Proc. R. Soc. London, Ser. A **231**, 505–514.

Envia, E., and Nallasamy, M. (**1999**). ''Design selection and analysis of a swept and leaned stator concept,'' J. Sound Vib. **228**, 793–836.

Ffowcs Williams, J. E., and Hall, L. H. (**1970**). ''Aerodynamic sound generation by turbulent flow in the vicinity of a scattering half-plane,'' J. Fluid Mech. **40**, 657–670.

Ffowcs Williams, J. E., and Hawkings, D. L. (**1969**). ''Sound generation by turbulence and by surfaces in arbitrary motion,'' Philos. Trans. R. Soc. London, Ser. A **264**, 321–342.

Fitzgerald, J. M., and Lauchle, G. C. (**1984**). ''Reduction of discrete frequency noise in small, subsonic axial-flow fans,'' J. Acoust. Soc. Am. **76**, 158–166.

Fukano, T., Takamatsu, Y., and Kodama, Y. (**1986**). ''The effects of tip clearance on the noise of low pressure axial and mixed flow fans,'' J. Sound Vib. **105**, 291–308.

Gerhold, C. H. (**1997**). ''Active control of fan-generated tone noise,'' AIAA J. **35**, 17–22.

Glegg, S. A. L., and Jochault, C. (**1998**). ''Broadband self-noise from a ducted fan,'' AIAA J. **36**, 1387–1395.

Gutin, L. (**1936**). ''On the sound field of a rotating propeller,'' *NACA TM 1195* (Translated in 1948 from Zh. Tekh. Fiz. **6**, 899–909).

Howe, M. S. (**1999**). ''Trailing edge noise at low Mach numbers,'' J. Sound Vib. **225**, 211–238.

Kaji, S., and Okazaki, T. (**1970**). ''Generation of sound by rotor–stator interaction,'' J. Sound Vib. **13**, 281–307.

Kemp, N. H., and Sears, W. R. (**1953**). ''Aerodynamic interference between moving blade rows,'' J. Aeronaut. Sci. **20**, 583–598.

Kemp, N. H., and Sears, W. R. (**1955**). ''Unsteady forces due to viscous wakes in turbomachines,'' J. Aeronaut. Sci. **22**, 478–483.

Lauchle, G. C., MacGillivray, J. R., and Swanson, D. C. (**1997**). ''Active control of axial-flow fan noise,'' J. Acoust. Soc. Am. **101**, 341–349.

Lewy, S. (**1992**). ''Theoretical study of the acoustic benefit of an open rotor with uneven blade spacings,'' J. Acoust. Soc. Am. **92**, 2181–2185.

Lighthill, M. J. (**1952**). ''On sound generated aerodynamically. I. General theory,'' Proc. R. Soc. London, Ser. A **211**, 564–587.

Longhouse, R. E. (**1976**). ''Noise mechanism separation and design considerations for low tip-speed, axial-flow fans,'' J. Sound Vib. **48**, 461–474.

Longhouse, R. E. (**1977**). ''Vortex shedding noise of low tip speed, axial flow fans,'' J. Sound Vib. **53**, 25–46.

Lowson, M. V. (**1965**). ''The sound field for singularities in motion,'' Proc. R. Soc. London, Ser. A **286**, 559–572.

Lowson, M. V. (**1970**). ''Theoretical analysis of compressor noise,'' J. Acoust. Soc. Am. **47**, 371–385.

Majumdar, S. J., and Peak, N. (**1998**). ''Noise generation by the interaction between ingested turbulence and a rotating fan,'' J. Fluid Mech. **359**, 181–216.

Morfey, C. L. (**1973**). ''Rotating blades and aerodynamic sound,'' J. Sound Vib. **28**, 587–617.

Mugridge, B. D., and Morfey, C. L. (**1972**). ''Sources of noise in axial flow fans,'' J. Acoust. Soc. Am. **51**, 1411–1426.

Quinlan, D. A. (**1992**). ''Application of active control to axial flow fans,'' Noise Control Eng. J. **39**, 95–101.

Quinlan, Q. A., and Bent, P. H. (**1998**). ''High frequency noise generation in small axial flow fans,'' J. Sound Vib. **218**, 177–204.

Schulten, J. B. H. M. (**1997**). ''Vane sweep effects on rotor/stator interaction noise,'' AIAA J. **35**, 945–951.

Sharland, I. J. (**1964**). ''Sources of noise in axial flow fans,'' J. Sound Vib. **1**, 302–322.

Subramanian, S., and Mueller, T. J. (**1995**). ''An experimental study of propeller noise due to cyclic flow distorsion,'' J. Sound Vib. **183**, 907–923.
Trunzo, R., Lakshminarayana, B., and Thompson, D. E. (**1981**). ''Nature of inlet turbulence and strut flow disturbances and their effect on turbomachinery rotor noise,'' J. Sound Vib. **76**, 233–259.
Tyler, J. M., and Sofrin, T. G. (**1962**). ''Axial flow compressor noise studies,'' SAE Trans. **70**, 309–332.
Wong, J., and Huang, L. (**2003**). ''Identification and control of noise sources in a small axial-flow cooling fan,'' Symposium on Fan Noise 2003, Senlis, France, 23–25 September.